

An Ising Hamiltonian Solver using Stochastic Phase-Transition Nano-Oscillators - Supplementary Information

S. Dutta^{1*†}, A. Khanna^{1†}, H. Paik³, D. Schlom³, A. Raychowdhury⁴,
Z. Toroczkai² and S. Datta¹

¹Department of Electrical Engineering, University of Notre Dame, Notre Dame, IN 46556, USA

²Department of Physics, University of Notre Dame, Notre Dame, IN 46556, USA

³Department of Materials Science and Engineering, Cornell University, Ithaca, NY 14853, USA

⁴School of Electrical and Computer Engineering, Georgia Institute of Technology, Atlanta, GA
30318 USA

† These authors contributed equally to this work

*Corresponding author email: sdutta4@nd.edu

Content:

- S1. Dynamical system theory for coupled PTNO network
- S2. Calculation of the perturbation-perturbation-vector (PPV)
- S3. Comparison between PTNO network and the Ising or XY-model
- S4. Calculation of oscillator phases
- S5. Optimization of coupling capacitance and noise
- S6. Comparison among LC, ring and phase-transition oscillators

S1. Dynamical system theory for coupled PTNO network

The Adler's Equation describes the evolution of the phase difference of a free-running sinusoidal oscillator (or LC oscillator) with respect to a sinusoidal (AC) injection locking signal. The generalised Adler's Equation (I) given by Eq. 1 in the main manuscript extends this to any non-linear oscillator with an arbitrary periodic injection locking signal. Analytical and numerical techniques to predict the locking behaviour for LC and ring oscillators have been shown (2) based on the Perturbation Projection Vector (PPV). The PPV tracks the excess phase delay generated in a free-running oscillator from a small current (or voltage) perturbation at the oscillating node. We numerically calculate the PPV ($\xi(t)$) from the impulse response of the PTNO through SPICE simulations (see Supplementary Section S2 for details). The phenomenon of injection locking involves a continuous perturbation from an input signal ($b(t)$) such as a sinusoidal signal with a fixed frequency. The excess phase delay of the oscillator due to this external perturbation signal can then be calculated by multiplying the PPV with the input signal. The excess phase delay generated over one time period is given by

$$g(\theta(t)) = \int_0^{2\pi} \xi(\theta(t) + \vartheta) b(\vartheta) d\vartheta$$

where $\theta(t)$ is the initial phase difference between the oscillator and injection locking signal. The integration is performed in the phase space over one oscillation period. For FHIL, we can write the generalised Adler's equation describing the rate of change phase difference between the oscillator and signal as

$$\frac{d\theta(t)}{dt} = -(f_{inj} - f_o) + f_o g(\theta(t))$$

or

$$\frac{d\theta(t)}{dt} = -(f_{inj} - n_H f_o) + K_{inj}^H \int_0^{2\pi} \xi(\theta(t) + \vartheta) \cos(\vartheta) d\vartheta$$

for $b(\vartheta) = V_{inj} \sin(\vartheta)$. Here, n_H is the n^{th} harmonic of the PTNO and $K_{inj}^H = 2\pi n_H f_o f_{inj} C_{inj} V_{inj}$.

This predicts the existence of a stable phase lock when $\frac{d\theta(t)}{dt} = 0$, or

$$g(\theta(t)) = K_{inj} \int_0^{2\pi} \xi(\theta(t) + \vartheta) \cos(\vartheta) d\vartheta = \frac{(f_{inj} - f_o)}{f_o}$$

The steady-state analysis produces two solutions for θ , one of which is stable. Note that for the producing a stable solution, the relative frequency difference between the oscillator and the injection locking signal must be smaller than the magnitude of $g(\theta)$ (see supplementary section S2 for details). In the case of SHIL, two stable solutions are produced. The corresponding "energy" or the Lyapunov function is obtained following the equation of a gradient system (3)

$$\frac{d\theta(t)}{dt} = -\frac{\partial E(\theta)}{\partial \theta}$$

Thus, the "energy" of a single injection locked oscillator is given by

$$E(\theta) = (f_{inj} - n_H f_0)\theta - K_{inj}^H \int_0^\theta \int_0^{2\pi} \xi(\phi + \vartheta) \cos(\vartheta) d\vartheta d\phi$$

The presence of one stable solution for FHIL and two stable solutions for SHIL is also predicted by the calculated energy landscape that shows a single energy well and double energy well for FHIL and SHIL, respectively (see Fig. 2(b) of main manuscript).

The gen-Adler equation is be further extended to describe the interaction between the pair of non-linear oscillators which results in a coupled oscillator system. We can write a coupled pair of differential equations as

$$\begin{aligned} \frac{d\theta_1(t)}{dt} &= -(f_2 - f_1) + f_1 g_1(\theta_1(t)) \\ \frac{d\theta_2(t)}{dt} &= -(f_1 - f_2) + f_2 g_2(\theta_2(t)) \end{aligned}$$

Where

$$g_i(\theta_i(t)) = \int_0^{2\pi} \xi(\theta_i(t) + \vartheta) I_{osc,j}(\vartheta) d\vartheta ; i, j = 1, 2 ; i \neq j$$

And $I_{osc,j}(\vartheta) = C_c \frac{dV_{osc}(\vartheta)}{d\vartheta}$ for capacitive coupling and $I_{osc,j}(\vartheta) = -\frac{V_{osc}(\vartheta)}{R_c}$ for resistive coupling.

Thus, overall, the dynamics of the network including injection locking and mutual coupling between oscillators can be written as

$$\begin{aligned} \frac{d\theta_i(t)}{dt} &= -(f_{inj} - n_H f_{o,i}) + K_{inj,i}^H \int_0^{2\pi} \xi_i(\theta_i(t) + \vartheta) \cos(\vartheta) d\vartheta \\ &\quad + f_0 \sum_{j=1, j \neq i}^N \int_0^{2\pi} \xi_i(\theta(t) + \vartheta) I_{osc,j} d\vartheta \end{aligned}$$

and corresponding “total energy“ or the global Lyapunov function of the system is then given by

$$\begin{aligned} E(\vec{\theta}) &= \sum_{i=1}^N (f_{inj} - n_H f_0)\theta_i - K_{inj}^H \sum_{i=1}^N \int_0^{\theta_i} \int_0^{2\pi} \xi_i(\phi + \vartheta) \cos(\vartheta) d\vartheta d\phi \\ &\quad - f_0 \sum_{i,j=1, i \neq j}^N \int_0^{\theta_i} \int_0^{2\pi} \xi_i(\phi + \vartheta) I_{osc,j} d\vartheta d\phi \end{aligned}$$

S2. Calculation of the perturbation-perturbation-vector (PPV)

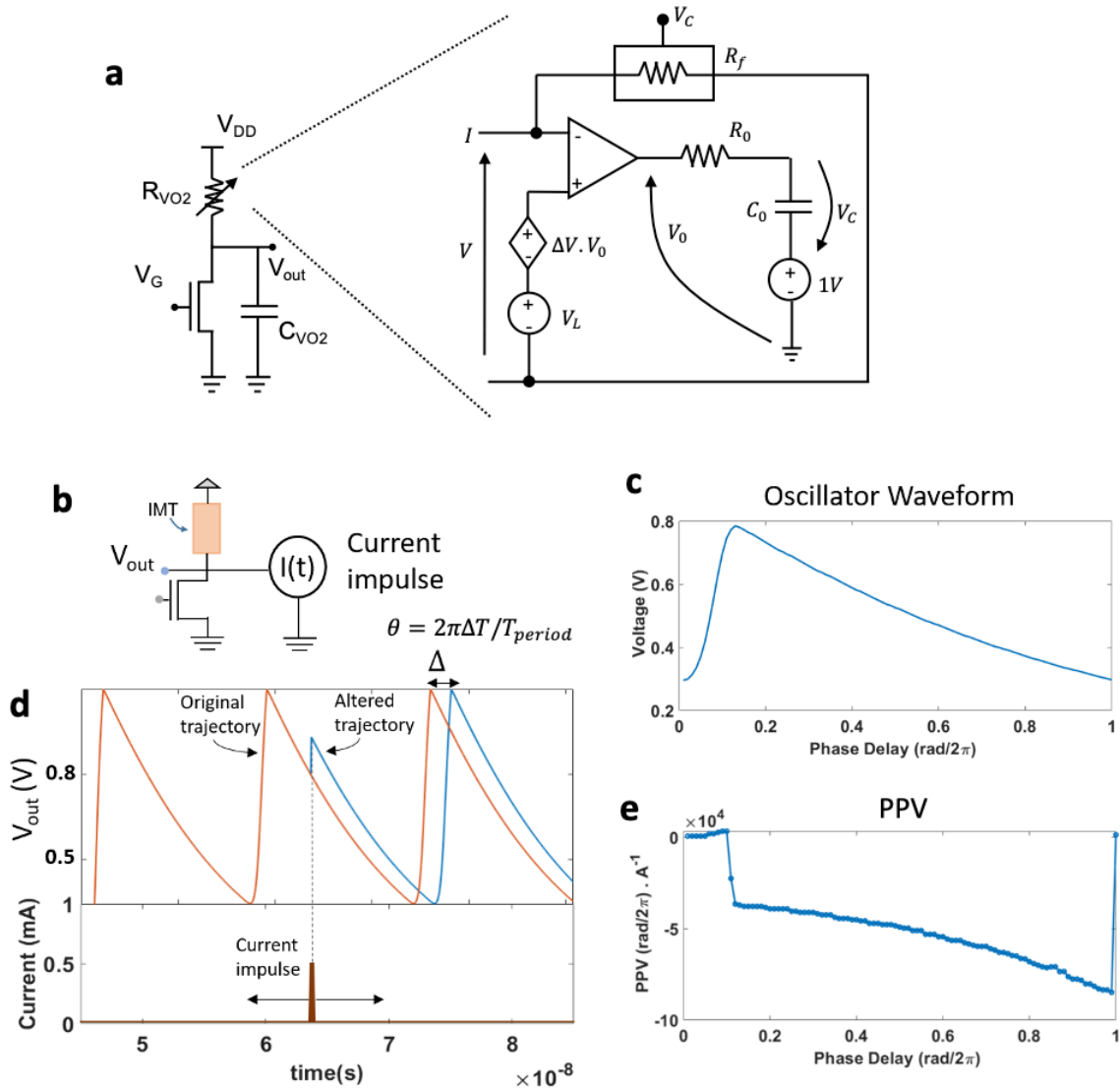


Fig. S1. Details of calculating the PPV for PTNO. (a) Compact SPICE circuit model for simulating a PTNO. The model VO₂ is based on a previous work (4, 5). (b) Schematic for the numerically calculating the PPV of IMT nano-oscillator. (c-e) Waveform of the non-linear phase transition oscillator and its corresponding PPV over one oscillation cycle.

The perturbation projection vector (PPV) is the phase response of an oscillator to an impulse current input normalized to the amount of injected charge and the oscillator frequency. We setup a SPICE circuit simulation to numerically calculate the PPV. A single IMT nano-oscillator consisting of a 2-terminal hysteretic phase transition device is placed in series with a n-channel MOSFET to create an oscillating waveform as shown in Fig. Fig. S1(a, b). An ideal current source $I(t)$ is connected to the oscillating node for producing a current impulse with a duration much smaller than the oscillator's time period. We sweep the delay of the perturbation over 100 steps covering one time period of the oscillation. For each delay, we compare the altered waveform (or

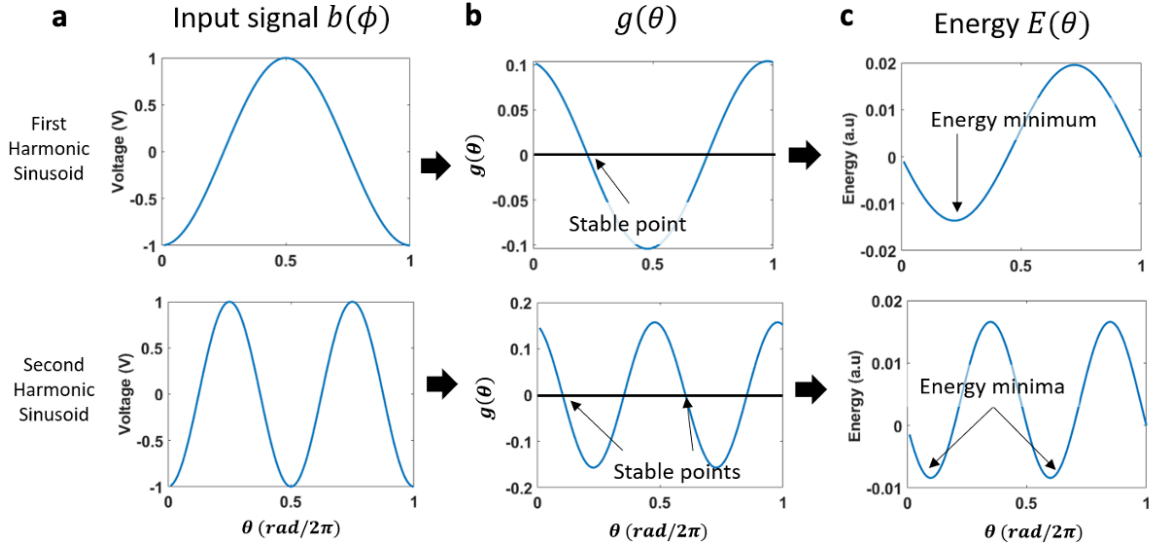


Fig S2. Calculating stable solutions and energy minima. (a) FHIL and SHIL input signal and corresponding (b) $g(\theta(t))$ showing one stable point and 2 stable points respectively. (c) Energy landscape for both FHIL.

trajectory) to the original unperturbed trajectory and measure the time difference ΔT between the two as shown in Fig. S1(d). The corresponding phase difference is measured as $\theta = 2\pi\Delta T / T_{period}$. The PPV is then calculated as below

$$PPV : \xi(\theta) = \frac{\theta}{\int I(t) dt}$$

Fig. S1(c) and (e) show the original waveform of the PTNO and its corresponding PPV. The excess phase generated over 1 oscillation cycle due to the injection locking signal is given by

$$g(\theta(t)) = \int_0^{2\pi} \xi(\theta(t) + \vartheta) \cdot b(\vartheta) d\vartheta$$

where $b(\vartheta)$ is the external injection locking signal. We show the calculated phase delay ($g(\theta)$) for first harmonic injection locking (FHIL) and second harmonic injection locking (SHIL), i.e for $b(\vartheta) = \sin(\vartheta)$ and $b(\vartheta) = \sin(2\vartheta)$, respectively as shown in Fig. S2(a).

From gen-Adler's equation

$$\frac{d\theta(t)}{dt} = -(f_{inj} - f_o) + f_o g(\theta(t))$$

the existence of a phase lock is predicted when $\frac{d\theta(t)}{dt} = 0$, or

$$g(\theta(t)) = K_{inj} \int_0^{2\pi} \xi(\theta(t) + \vartheta) \cdot \cos(\vartheta) d\vartheta = \frac{(f_{inj} - f_o)}{f_o}$$

Assuming zero frequency offset, this is the phase delay corresponding to the zero crossings of $g(\theta)$ as shown in Fig. S2(b). For FHIL, there are two zero crossings of which only one is a stable phase locking (at $\theta \cong 0.4\pi$), when $\frac{d^2\theta(t)}{dt^2} = \frac{dg(\theta(t))}{dt} = -ve$, i.e. where the acceleration of the phase delay change is negative. For SHIL, there are 2 such stable points at $\theta \cong 0.2\pi$ and $\theta \cong 1.2\pi$ as shown in Fig. S2(b).

We can also calculate the energy of the dynamical oscillator – injection locked system from

$$\frac{d\theta(t)}{dt} = -\frac{dE(\theta)}{d\theta}$$

From the Gen-Adler equation above (assuming zero frequency mismatch), the energy is given by

$$E(\theta) = f_o \int_0^{\theta} g(\theta) d\theta = K_{inj} \int_0^{2\pi} \xi(\theta(t) + \vartheta) \cdot \cos(\vartheta) d\vartheta = \frac{(f_{inj} - f_o)}{f_o}$$

which is be numerically calculated as shown in Fig. S2(c) and Fig. 2(b) of the main text and agrees well with experimental results.

S3. Comparison between PTNO network and the Ising or XY-model

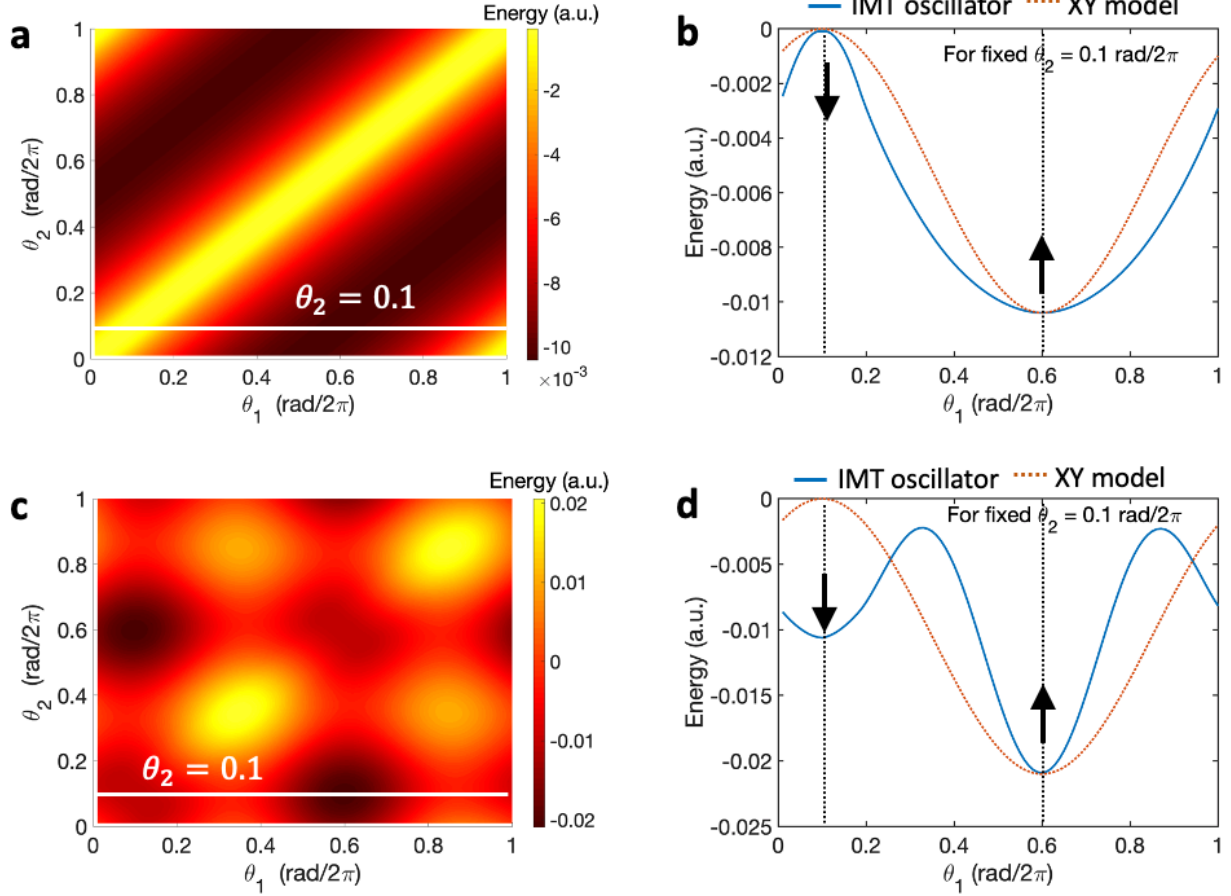


Fig S3. Comparison with the Ising model and the XY model (a, c) Two oscillator energy landscape shown without and with second harmonic injection locking, respectively. **(b)** Energy landscape due to capacitive coupling interaction between two PTNOs is similar to interaction energy of the anti-ferromagnetic coupled XY model with a minimum at $(\theta_1 - \theta_2 = \pi)$. **(d)** SHIL introduces a local minimum at $(\theta_1 - \theta_2 = 0)$ which was previously a maximum, however the shape of energy landscape around global minimum $(\theta_1 - \theta_2 = \pi)$ remains the same as before.

The XY model is a generalization of the Ising model where each spin is represented not by a discrete variable $s_i \in \{-1, +1\}$, but rather by continuous vector $s_i = (\sin(\theta_i), \cos(\theta_i))$. The interaction energy between two spins in the XY model is given by

$$E_{ij} = -J_{ij} s_i \cdot s_j = -J_{ij} \cos(\theta_i - \theta_j)$$

This becomes equivalent to the Ising model when $(\theta_i - \theta_j) \in \{0, \pm\pi\}$, i.e. when the spins are completely parallel or antiparallel with each other. As shown in Fig. S3(b), the two-oscillator interaction energy landscape closely resembles the XY-model especially around the neighbourhood of the minima or maxima points, i.e. $(\theta_1 - \theta_2) \in \{0, \pm\pi\}$ and become equal to the

Ising model at $(\theta_i - \theta_j) \in \{0, \pm\pi\}$. Upon introducing the SHIL, the energy landscape is changed. As shown in figure Fig. S3(d), this introduces a local minimum at $\theta_1 - \theta_2 = 0$. Hence, the shape of the energy landscape deviates from the XY model around $\theta_1 - \theta_2 = 0$ and remains equivalent to the XY model around the global minima ($\theta_1 - \theta_2 = \pi$). However, it remains equal to the Ising model at $(\theta_i - \theta_j) \in \{0, \pm\pi\}$.

S4. Calculation of oscillator phases

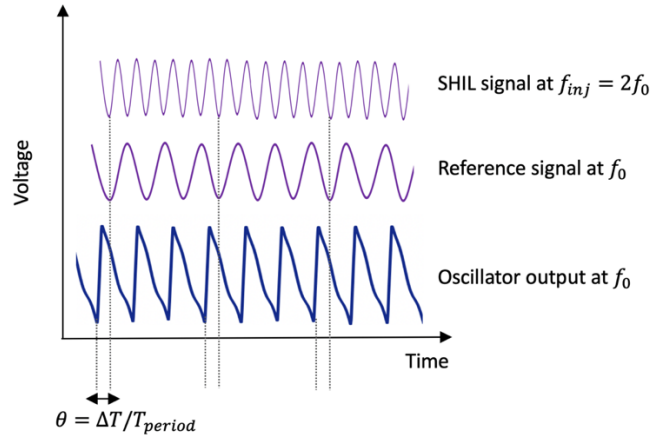


Fig. S4. Schematic showing the calculation of the phase of an IMT nano-oscillator. The phase is calculated with respect to a reference sinusoidal signal at the same frequency as the oscillator. The minima points in the voltage waveforms are considered for the phase calculation.

S5. Optimization of coupling capacitance and noise

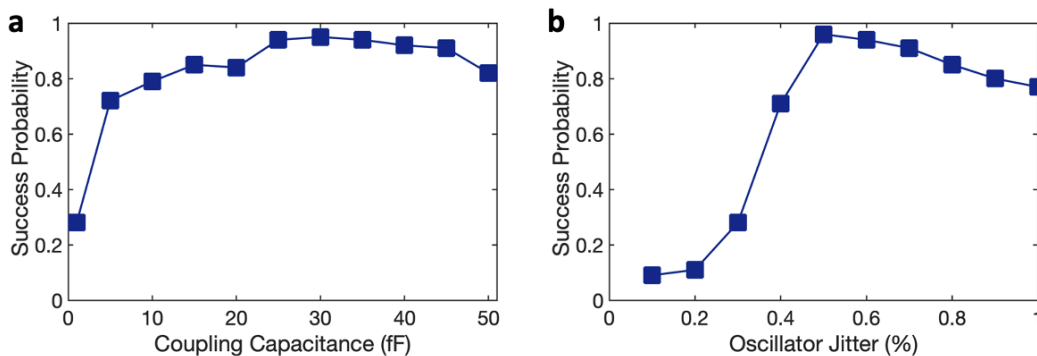


Fig. S5. Optimization of coupling capacitance and oscillator jitter noise. Success probability of solving the Max-CUT problem for a mobius ladder graph of 10 nodes with IMT nano-oscillators is shown as a function of varying (a) coupling capacitance and (b) oscillator jitter noise.

The energy landscape of the oscillator network is sensitive to the choice of simulation parameters such as capacitive coupling and stochasticity in the system. In our simulations, we set the parameters such as C_S , C_{inj} , R_m and R_i as described in the Method section of the main text. The amplitude of the injection locking signal is chosen to be sufficient enough to reliably binarize the oscillator phases. The interaction energy between the oscillators is modulated by the value of the coupling capacitance C_C and we find the optimum value for this interaction by measuring the success probability of a 10 node mobius ladder Max-cut problem for different values of capacitance as shown in Fig. S5(a). Lower coupling strength means that the interactions between the oscillators are too weak, resulting in the energy difference between the different Ising spin configurations being smaller, leading to a lower chance of the oscillators to find the minimum energy configuration and hence a lower success probability. Conversely, if the interaction energy is too strong compared to the injection locking strength, then the binarization of the oscillator phases is reduced resulting in a wider distribution in the phase space. This apparent destruction of the ‘up’ and ‘down’ spin nature of the phases in some simulation leads to a lower overall success probability. We found that a coupling capacitance strength of $C_C = 30 \text{ fF}$ was an optimum value to achieve maximum success probability and is approximately 16% of the total VO₂ capacitance C_S . We used this coupling capacitance value for all our simulations up to 200 oscillators. Stochasticity is the second parameter that can greatly affect the likelihood of the oscillator network to escape the local energy minima and reach the global optimum energy configuration. We introduce stochasticity in the form of oscillator jitter phase (or frequency) jitter. Too little stochasticity would mean the system gets stuck in local minima and is not able to jump out to reach the global minimum. On the other hand, a very large amount of intrinsic noise would cause the system to jump out of the global energy minimum configuration even at highest injection locking leading to lower probability of success when the phase is read-out. We varied the amount of noise for a 10-oscillator system and found that a 0.5% oscillator jitter was the ideal amount of noise to achieve maximum success probability while solving a mobius ladder Max-Cut graph (Fig S5(b)). We used this amount of oscillator jitter for all our simulations up to 200 oscillators.

S6. Comparison among LC, ring and phase-transition oscillators

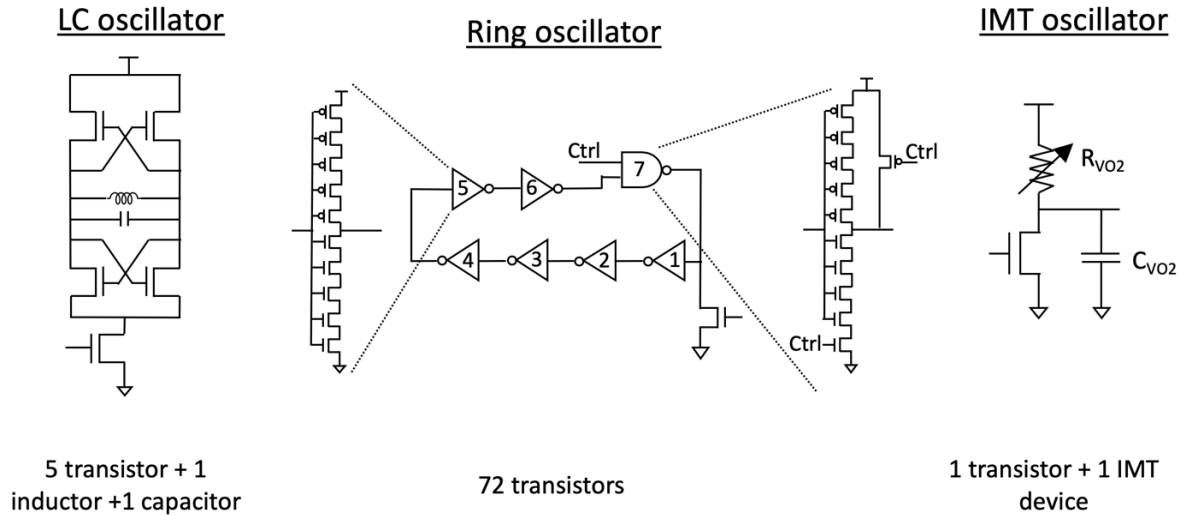


Fig. S6. Comparison between LC oscillator, ring oscillator and PTNO.

Fig. S6 shows the circuit schematic of an LC oscillator (6), a seven-stage ring oscillator (7) and the PTNO. The inductor in an LC oscillator takes up most of the area, close to 0.1 mm^2 (8). The ring oscillator has a comparatively lower area. Ref. (7) reports a unit cell area of $950 \mu\text{m}^2$. In contrast, our PTNO comprises a transistor and a scaled VO_2 device which takes up orders of magnitude lower area (4).

References

1. P. Bhansali, J. Roychowdhury, Gen-Aadler: The generalized adler's equation for injection locking analysis in oscillators. *Proc. Asia South Pacific Des. Autom. Conf. ASP-DAC*, 522–527 (2009).
2. X. Lai, J. Roychowdhury, Analytical equations for predicting injection locking in LC and ring oscillators. *Proc. Cust. Integr. Circuits Conf.* **2005**, 454–457 (2005).
3. J. L. van Hemmen, W. F. Wreszinski, Lyapunov function for the Kuramoto model of nonlinearly coupled oscillators. *J. Stat. Phys.* (1993), doi:10.1007/BF01048044.
4. S. Dutta, A. Parihar, A. Khanna, J. Gomez, W. Chakraborty, M. Jerry, B. Grisafe, A. Raychowdhury, S. Datta, Programmable coupled oscillators for synchronized locomotion. *Nat. Commun.* (2019), doi:10.1038/s41467-019-11198-6.
5. P. Maffezzoni, L. Daniel, N. Shukla, S. Datta, A. Raychowdhury, Modeling and Simulation of Vanadium Dioxide Relaxation Oscillators. *IEEE Trans. Circuits Syst. I Regul. Pap.* **62**, 2207–2215 (2015).
6. T. Wang, J. Roychowdhury, in *Lecture Notes in Computer Science (including subseries Lecture Notes in Artificial Intelligence and Lecture Notes in Bioinformatics)* (2019).
7. I. Ahmed, P.-W. Chiu, C. H. Kim, in *Symposia on VLSI Technology and Circuits* (2020).

8. Z. Zahir, G. Banerjee, in *2016 IEEE Asia Pacific Conference on Circuits and Systems, APCCAS 2016* (2017).